Check for updates

Development of flax/basalt/PA11 bio-composites: optimal formulation and modelling of the quasi-static behaviour

Wassim Guerfala[1,2]*, Patrick Rozycki[1] and Christophe Binetruy[1]

[1]Institut de recherche en génie civil et mécanique, UMR CNRS 6183, Ecole centrale Nantes, Nantes Université, Nantes, France, [2]Department Body in White Research and Innovation Unit, Bertrandt, Vélizy, France

Environmental impact is becoming increasingly important in the automotive industry, with car manufacturers looking to reduce CO_2 emissions through cleaner engines and structural weight reduction. Composite materials offer an excellent alternative to standard steels with significant weight reduction and the ability to produce functional parts (Rangappa et al., Polymer Composites, 2022,43, 645−691), (Jeyaguru et al., Polymer Composites, 2022, 43, 3902−3914), (Sanjay et al., Journal of Cleaner Production, 2018, 172, 566−581). The main objective of this study is to investigate the potential of a new and unique hybrid bio-composite material combining flax and basalt fibers and PA11 polymer. This material design is studied with the idea of reducing the moisture sensitivity, variabilities, and uncertainties of vegetal fibers by the presence of basalt fibers. The first step consists of developing a new hybrid composite material and studying its quasi-static mechanical behaviour when subjected to different humidity levels. Then, a multi-scale non-linear homogenization approach is proposed to support the interpretation of the characterization test results. The experimental results show the benefits of the hybridization. In fact, the hybrid composite is 20% stiffer than the flax/PA11 composite, 8% lighter than the basalt/PA11 composite and has a reduced dispersion of its mechanical properties, 52% lower than the flax/PA11 composite. Considering the promising properties of the hybrid composite, we have investigated the possibility of developing the front hood of a sports car using this material. The first results highlight a potential mass gain of 18% at iso-performance with the original front hood. The following steps will be devoted to the numerical and experimental validation.

KEYWORDS

composite materials, natural fibers, hybrid composite, homogenization, thermo-compression

Introduction

The application of composite materials remains limited in the automotive industry due to various technical, economic, and environmental constraints. Knowledge of the technical aspects of manufacturing (processes and production rate), the mechanical behaviour of these heterogeneous materials (behaviour law and simulation tools) and their lifespan are still insufficient for mass production. On the economic aspect, the high price of fibers, such as carbon fibers, and the high manufacturing cost related to cycle time are the main obstacles to developing these materials. Furthermore, the environmental impact became increasingly

critical with new European regulations for reducing the CO_2 emission and the Carbone footprint of the life cycle automotive structures. The main objective of this research is to define a new concept for semi-structural automotive parts (hood, door, dashboard …) that can meet the various industrial requirements while respecting environmental regulations. Therefore, the initial work has focused on selecting materials from a wide range of vegetal fibers and bio-sourced polymers with suitable properties. Then, a focus was made on the characterization of hybrid composite materials through various quasi-static mechanical tests at different humidity levels. Hybridization is a frequently employed process to create intermediate properties between the two original materials (Swolfs et al., 2019).

Hybridization can result in a trade-off between mechanical properties and economic cost in order to meet the application requirements. Several recent studies show that the mechanical properties can be adapted by using hybridizations based on basalt fiber laminates with other natural fibers (Raponi et al., 2022), (Fargassa et al., 2018), (Petrucci et al., 2013), intending to provide a more durable material. These studies mainly focused on the impact and mechanical characterization properties of a basalt/flax hybrid composite. All the composites involved were thermoset composites (epoxy, vinylester) with laminate hybridization. This study analyzed an original combination of flax and basalt fibers and a thermoplastic matrix (PA11) with a fabric scale hybridization by co-weaving. This work focuses on the effect of hybridization on mechanical properties. Then the effect of hygrometry on the evolution of the mechanical behavior of the composite (with three levels of hygrometry). Finally, the hybridization interest in reducing the dispersion of the mechanical properties of the studied material.

Various bio-composite materials based on natural fibers and bio-sourced matrices are used in industry (Nasimudeen et al., 2021), (Mohit et al., 2022), (Jeyaguru et al., 2022b) motivated by mass reduction (Jeyaguru et al., 2022c), (Jeyaguru et al., 2022d), (Chandrasekar et al., 2022), (Jeyaguru et al., 2023) environmental impact limitation (Mohit et al., 2022), (Chandrasekar et al., 2020), (Baley et al., 2017), (Fragassa et al., 2015) good recyclability (Bourmaud and Baley, 2007).The choice of these materials is essential and is linked to the final properties required for the semi-structural parts. Therefore, different matrices and fibers have been compared according to manufacturing constraints, processing conditions, environmental impact, and economic requirements.

The hybridization concept uses two or more fibers reinforcing the same matrix. It provides sufficient flexibility to design the optimal material (Senthilkumar et al., 2022), (Athith et al., 2018), (Kumar et al., 2020). The main idea is to mitigate the weaknesses of one of the fibers while keeping the advantages of the other (s) (Senthilkumar et al., 2019), (Shahroze et al., 2019), (El Hadi et al., 2019). This composite material offers many advantages but requires in-depth study to define the best combination of compatible fibers (Shahroze et al., 2019). The mechanical properties of the hybrid composite (fiber A and fiber B) are often the weighted average of the respective mechanical properties of both fibers. A better combination can create a synergetic effect that improves the hybrid composite properties compared to composites reinforced with only one type of fibre (Senthilkumar et al., 2019), (Shahroze et al., 2019).

There are two leading families of fibers: synthetic and natural (mineral fibers, plant fibers and animal fibers) (Swolfs et al., 2014). Natural fibers, whose mechanical properties are similar to those of glass fibers were studied. Mineral fibers have good mechanical and thermal properties due to their chemical composition based on silicon (e.g., asbestos, basalt). Plant fibers are available in a wide range depending on the type of plant and its origin (leaves, stems, seeds or fruits) (Baley et al., 2017), (Bourmaud and Baley, 2009).

A first selection of natural fibres was made based on studies of bio-composite materials and their application fields (Baley et al., 2017), (Fragassa et al., 2015). The industrial aspect of fibre production (quantity and quality of the products) represented an essential factor in this selection. The following fibres were selected: hemp, sisal, ramie, jute, flax and basalt. In the second step, specific constraint functions were defined, which reflect the industrial requirements: structural lightness, mechanical performance, cost, environmental impact and durability. It was decided to select flax and basalt as fibre reinforcement and a PA11 matrix from Arkema (Fragassa et al., 2015). These different constituents are compatible and have complementary mechanical properties. Flax fiber has good mechanical properties (Baley et al., 2017), (Baley and Bourmaud, 2014a)and low density (1.4 g/cm³) (Baley et al., 2017), while basalt fiber provides high stiffness (Young's modulus of 93 GPa) (Baley et al., 2017), high moisture resistance (water absorption rate of 0.03%) (Baley et al., 2017) and excellent temperature resistance (maximum application temperature: 850°C) (Baley et al., 2017). The choice of a thermoplastic matrix and natural fibers improves the recyclability of this hybrid bio-composite.

This article is structured as follows. First part concerns the results of the experimental study of the developed materials, basalt/PA11, flax/PA11 and hybrid5050/PA11 for different directions (0°/45°/90°). The second part concerns the moisture influence on the evolution of the mechanical behaviour of materials since both the flax fiber and the PA11 matrix are sensitive to moisture (Bourmaud and Baley, 2009), (Baley and Bourmaud, 2014a) and (Destaing et al., 2016). As this hybrid material is new, the interpretation of the experimental results is accompanied by the micromechanical analysis of the representative volume element (RVE) of the hybrid composites using the finite element method. To this end, the computational model uses Multiscale Designer (Altair) to predict the mechanical response of different RVEs beyond elastic regimes to understand the effects of flax fiber variability, its hybridization with basalt fibers and the influence of moisture on macroscale properties. The predictions are compared with experimental results.

Materials and methods

In this research work, the mechanical behaviour of the thermoplastic matrix PA11 and the composite materials flax/PA11, basalt/PA11 and hybrid5050/PA11 was investigated at three humidity levels (RH0, RH50 and RH85) and the ambient temperature of 23°C. The fibre distribution for the hybrid5050/PA11 composite is 50% flax fibre and 50% basalt fibre. The flax fibres used were supplied by the company Depestele in France, the basalt fibres were provided by the company Isomatex in Belgium and the PA11 polyamide matrix was developed by Arkema in France.
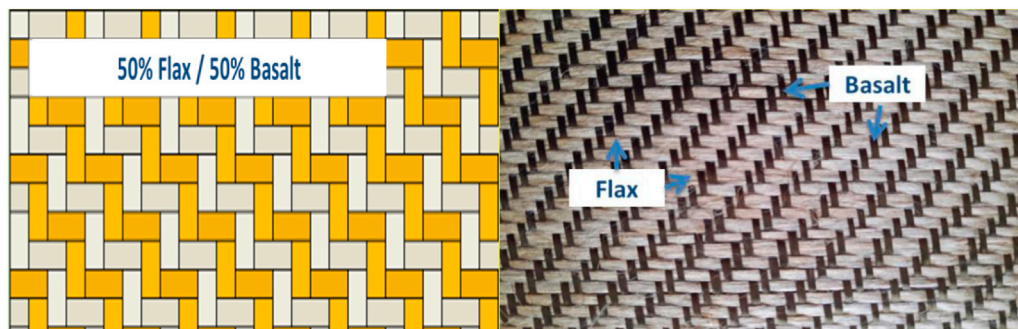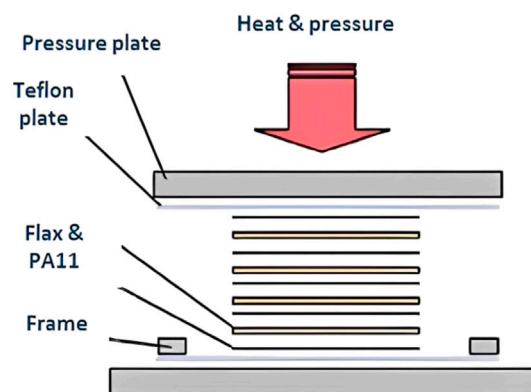
FIGURE 1
Hybrid5050/PA11 fabric Twill2X2.

FIGURE 2
Hydraulic press SCAMEX.

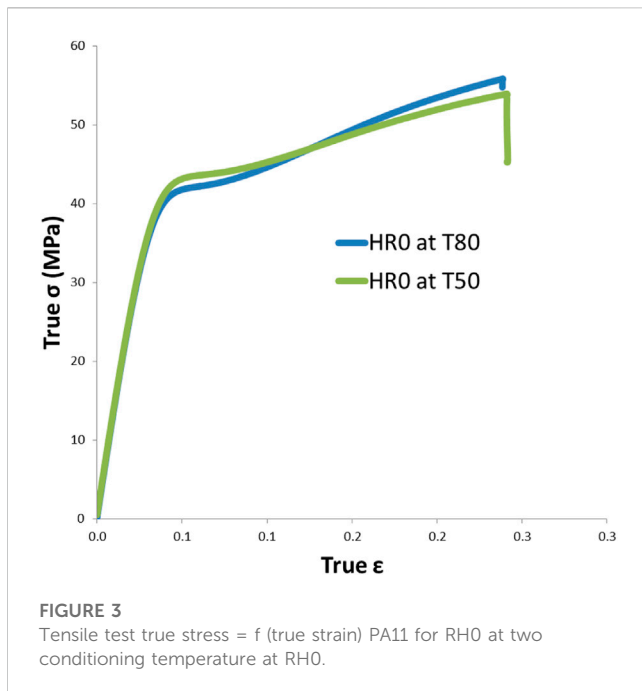Depestele weaved together the flax and basalt fibres to get the hybrid composite hybrid5050/PA11 (Figure 1).

Table 1 shows the mechanical properties of the PA11 matrix, flax and basalt fibers. The indices 1, 2, and 3 refer to the principal axes of the fiber, with axis 1 referring to the fiber axis (Nasimudeen et al., 2021).

Fabrication of composites

The choice of manufacturing depends on the selected materials' characteristics and the application's constraints. There is a wide variety of manufacturing processes for composite materials (Swolfs et al., 2019); each technology depends on several parameters. Indeed, the melting temperature, matrix viscosity, fiber length, thermal resistance, or geometric complexity of the manufactured parts must be considered. The thermo-compression process was chosen because of the matrix's thermoplastic nature, the flax fibre's temperature sensitivity and the short cycle time compatible with automotive production. It was applied for the different composite materials; flax/PA11 (twill, 4 plies, 2 mm thick, Vf 42%), basalt/PA11 (UD, 8 plies, 4 mm thick, Vf 27%) and hybrid5050 (twill, 4 plies and 2 mm thick, Vf 33%).

Thermo-compression allows forming composite parts with prepregs by combining pressure and temperature for a relatively short cycle time (Baley and Bourmaud, 2014b). An experimental study has defined the thermo-compression parameters (Supplementary Figure S1). The temperature is maintained at 220°C for 3 min during the heating phase and 23°C for 5 min during the cooling phase. The material is kept under a pressure of 5 bars during heating and 3 bars during cooling. The objective is to ensure proper impregnation of the fibers without risking the degradation of the flax fibers. A pre-drying phase of the fabrics was carried out to reduce the hygrometric effect on the prepreg impregnation quality and improve the composite's desorption (Barbulée et al., 2014).

FIGURE 3
Tensile test true stress = f (true strain) PA11 for RH0 at two conditioning temperature at RH0.

1. The first composite plates were produced by thermocompression with a hydraulic press SCAMEX of 75 tons of clamping, equipped with heated platens of 1 m² (Figure 2)

The final panels have been manufactured using industrial methods to consider the imperfections inherent in this type of production. The specimens were then cut out using a water jet. For composites, parallelepiped specimens were used. The specimens' dimensions are as follows: 2 mm thick, 25 mm wide and 250 mm long overall, they are in accordance with ISO 527 standard (the equivalent of ASTM D638 for tensile testing of reinforced and unreinforced polymers). The specimens used for the quasi-static tests of the PA11 thermoplastic matrix are of the dumbbell type. Their dimensions are defined as follows: 4 mm thick, 10 mm wide and a zone of interest of length 80 mm. The specimens were manufactured by the extrusion method by the a polymer materials laboratory.

Moisture absorption and desorption test

Given the sensitivity of the materials studied (thermoplastic matrix and vegetal fibers) to humidity (Bourmaud and Baley, 2009), (Barbulée et al., 2014), three standard levels of hygrometry (RH0—dry climate, RH50 - standard climate and RH85—humid climate) were analyzed for the matrix and composites in order to evaluate their effect on mechanical properties.

First, it was necessary to identify two experimental protocols: the first concerns the drying of the material, which allows a return to a dry state (RH0). The second is designed to ensure the samples are returned to a moist environment (RH50 and RH85). In both cases, gravimetric measurements were carried out to monitor the evolution of the specimen masses and determine the days required to dry or age the specimens. In order to return the material to a dry state,

samples were placed in an oven (Binder VD-115 equipped with a Vaccubrand PC3001 pumping unit) under vacuum at 80°C. This temperature was chosen in accordance with the instructions of the matrix supplier and the data reported in the literature on the thermal resistance of the flax fibers (no impact on their mechanical properties) (Bourmaud and Baley, 2009), (Barbulée et al., 2014). For ageing at RH50 and RH85, samples were placed in a climatic chamber (BINDER KMF115) at 80°C, the same temperature for drying and ageing in accordance with supplier's instructions. Some mechanical tensile tests were performed to verify that the drying temperature processes did not affect the mechanical behaviour of the composites (Figure 3).

In order to maintain the moisture content of the different materials during the characterization tests, the specimens were packed in batches of five in specific bags.

The moisture variation Mt is calculated using

$$M_t = \frac{m_t - m_0}{m_0} \qquad (1)$$

With m_0 initial mass, m_t sample mass

Gravimetric measurements were carried out on each material studied to follow the sample mass's evolution during conditioning. These measurements allow determining the variation of the humidity Mt for each material and identifying the time required for desiccation and sorption. Figure 4 shows the Mt's evolution and the humidity sensitivity (RH0, RH50 and RH85) for each material.

As shown in Figure 4, the basalt/PA11 composite has the highest moisture resistance and a shorter drying time than the flax/PA11 composite. The humidity ratio of the basalt/PA11 composite (0.5%) is relatively low compared to that of the flax/PA11 composite (3.6%). As expected, the hybrid5050/PA11 composite is intermediate in moisture resistance (2.32%) between the flax/PA11 and basalt/PA11 composites.

The moisture variation for RH50 plotted in Figure 4 shows a significant difference between the composites Basalt/PA11 (0.42% moisture content) and Lin/PA11 (2.22% moisture content); in fact, the basalt fibers are mineral fibers and have excellent moisture resistance (Raponi et al., 2022), (Fargassa et al., 2018). Regarding the hyb5050/PA11 composites, the moisture uptake (1.33%) remains lower than that of flax, indicating that the hybridization allows reducing the moisture sensitivity. Similarly, for RH85 in Figure 4, the same behavior is observed; the basalt has the lowest moisture content (0.83%), while that of the flax/PA11 composite (4.89%). The 5,050/PA11 hybrid shows 37% less moisture than the flax/PA11 composite.

Mechanical tests

The main objectives of the experimental phase were to identify the mechanical characteristics (Young's modulus, Shear modulus, Poisson's ratio, strength and strain at failure . . .) of the PA11 matrix and the composites flax/PA11, basalt/PA11 and hybrid50/50. Then to understand the evolution of their mechanical behavior according to the different humidity ranges RH0, RH50, and RH85 the quasi-static tensile and in-plane shear tests were carried out on a universal testing machine (INSTRON 5584), according to the ISO527 (ASTM
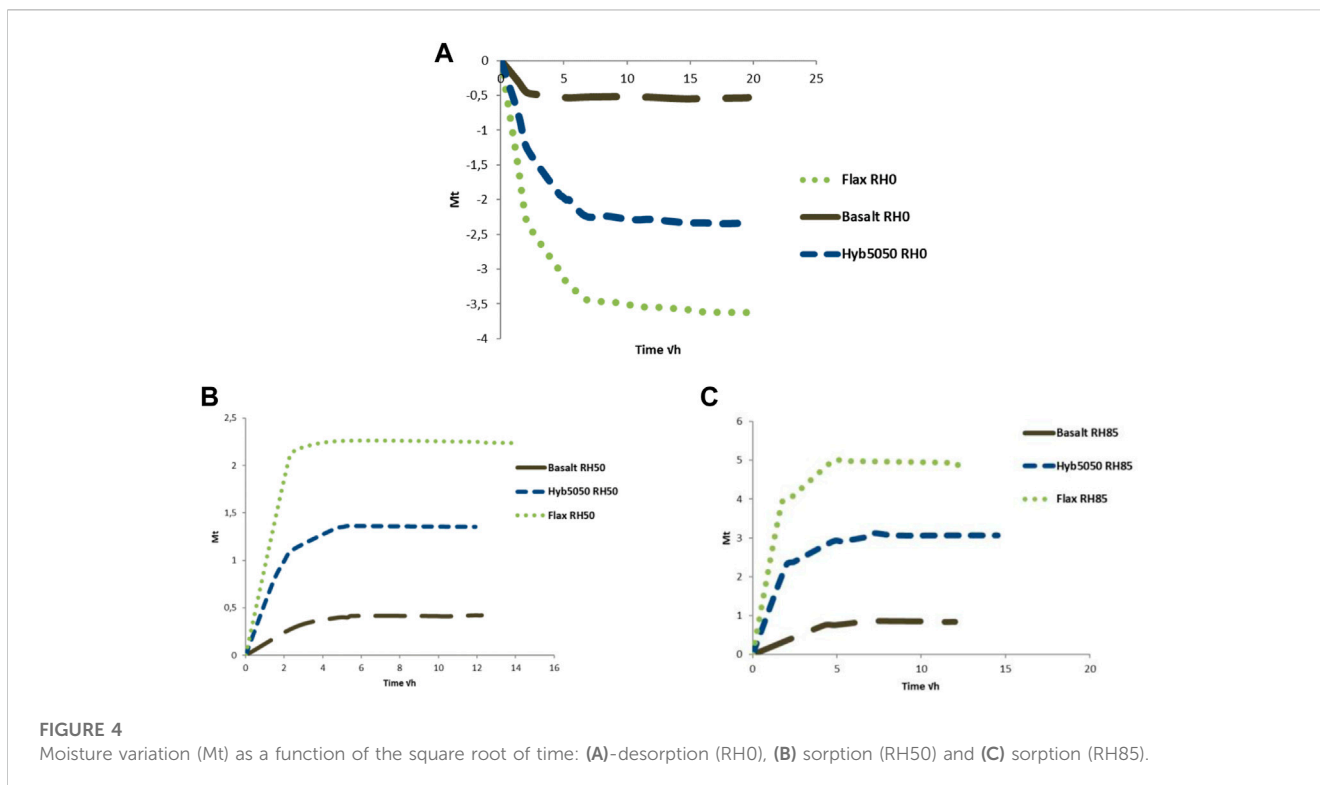
FIGURE 4
Moisture variation (Mt) as a function of the square root of time: **(A)**-desorption (RH0), **(B)** sorption (RH50) and **(C)** sorption (RH85).

D3039). The samples' dimensions are selected per the ISO 527 standard.

Quasi-static tests have been carried out in the dry state RH0 at ambient temperature(+23°C) and for different directions (0°/45°/ 90°). The choice of the hygrometry level was made to eliminate their effect on the mechanical behaviour of the composite, as flax fibers are sensitive to humidity and high temperature (Baley et al., 2017), and to understand the impact of the hybridization on the mechanical properties and mechanical behaviour of the hybrid5050/ PA11 material. The 0° orientation provides the longitudinal mechanical properties, the 45° orientation gives the shear properties and the 90° orientation provides the transverse mechanical properties of the composite. The second part of the experimental study highlights the effect of humidity for three humidity levels, RH0, RH50, and RH85, for the composite materials basalt/PA11, flax/PA11 and hybrid 5,050/PA11 as well as for the PA11 matrix.

Five samples were used for each of the tests reported in Supplementary Table S2 to ensure the reproducibility of the results.

A digital image correlation (DIC) method has been adopted to determine the strain field of the specimens. A high-resolution camera (STEMMER GT6600) is used to capture images during the tensile test, which are then processed using the VIC-2D software to calculate the strain field.

Analysis of the monotonic tensile tests provides the stiffness, strength and deformation at the failure of these materials. Due to their geometrical symmetries, unidirectional composite laminates are considered to be transversely isotropic materials (Baley et al., 2005). This hypothesis allows to simplify the relationships between stresses and strains for the different orientations. The calculated stresses and strains are local and are extracted from the quantities

measured in the global machine plan (Supplementary Figure S2). Supplementary Table S3 shows the quantities calculated as a function of the different laminates in the global coordinate system $(O, \vec{x}_1, \vec{x}_2, \vec{x}_3)$, the tensile test being performed in the $\vec{x}_1$ direction.

Experimental study

Figure 5 compares the different mechanical behaviors of the flax/ PA11, basalt/PA11 and hyb5050/PA11 composites. True stresses were calculated to take into account the potential effects of large deformations. The true stress σ and strain ε are determined from:

$$\sigma = \sigma_n (1 + \varepsilon_n) \qquad (2)$$

$$\varepsilon = ln (1 + \varepsilon_n) \qquad (3)$$

$$\varepsilon_n = \frac{l - l_0}{l_0} \qquad (4)$$

$$\sigma_n = \frac{F}{S_0} \qquad (5)$$

ε_n: nominal strain σ_n: nominal stress
F: applied force S_0: samples initial section
l: samples length l_0: samples initial length

The basalt/PA11 composite is stiffer than the hybrid 5,050/ PA11 and flax/PA11 composites for the 0° direction due to the relatively high mechanical properties of the basalt fiber (Singha, 2012) compared to the flax fiber (Baley et al., 2017). Furthermore, the basalt/PA11 composite is unidirectional, and the hybrid5050/ PA11 and flax/PA11 composites are balanced. The deformation of the basalt composites is relatively higher than that of the hybrid

FIGURE 5
True stress vs. true strain in the global coordinate system for the flax/PA11, Hyb5050/PA11 and basalt/PA11 composites for RH0 and 0˚, 45˚, and 90˚ at 23˚C.

FIGURE 6
Global true stress vs. true strain for tensile testing of flax/PA11 0˚ for RH0 at 23˚C.

5,050/PA11 and flax/PA11 composites for the different directions (0° and 90°). As conclusion, the hybridization has improved the mechanical characteristics of the hybrid 5,050/PA11 *versus* he flax/PA11 composite. Figure 5 shows that the hybrid composite is 20% stiffer than the flax composite. As expected, the Young modulus E22 of the unidirectional basalt/PA11 is significantly lower than the hybrid5050/PA11 and flax/PA11 woven composites (Figure 5). Also, the longitudinal and transverse Young's moduli of the 5,050/PA11 and Flax/PA11 are very similar because they are made from balanced twill fabrics. The different mechanical properties

of the studied composites are reported in Table 3. It is important to emphasise that it is possible to have a more consistent comparison if fibre content Vf for the hybrid5050/PA11 and flax/PA11 composites were the same. In fact, the fibre content for the different composites: flax/PA11 (Vf 42%), basalt/PA11 (Vf 27%) and hybrid5050/PA11 (Vf 33%) are different. This difference in fibre content is due to the process of powdering the fabric during the pre-impregnation manufacturing (50% by weight for the fibres, 50% by weight for the matrix). The hybrid5050/PA11 composite would have better mechanical properties with a higher fibre content, thus highlighting the interest in hybridization.

Figure 6 shows the typical dispersion of the mechanical behaviour for the flax/PA11 composite. This dispersion is essentially due to the plant nature of the flax fibers. Indeed, the mechanical characteristics of flax fibers depend on the nature of the fibers, the growth conditions (temperature and humidity), and the treatment carried out to process these fibers (Baley et al., 2017).

Dispersions are defined by:

$$Dispersion = \frac{standard\ deviation}{Main\ value} \times 100 \qquad (6)$$

The hybridization of flax fibers with basalt fibers reduced the scatter of the mechanical properties of the flax/PA11 composite. As a result, the hybrid5050/PA11 composite shows a lower dispersion of Young's modulus compared to both basalt/PA11 and flax/PA11 composites for the different directions (0˚, 45˚ and 90˚) as shown in Figure 7. Also, the dispersion of the different mechanical properties is more pronounced for the 45˚ direction compared to the 0˚ and 90˚ directions. Although basalt, due to its chemical composition and manufacturing
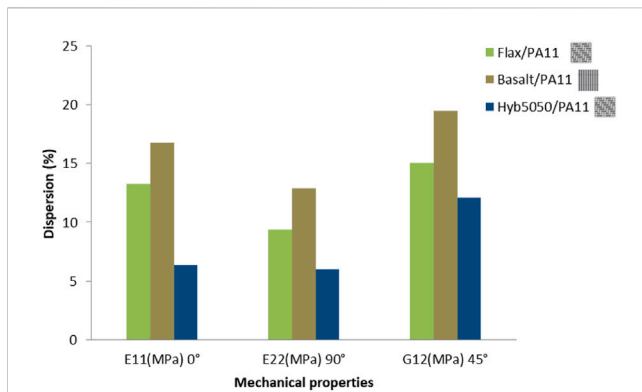
FIGURE 7
Mechanical property dispersion for basalt/PA11, flax/PA11 and hybrid5050/PA11 composites for directions 0°, 45°, and 90°.
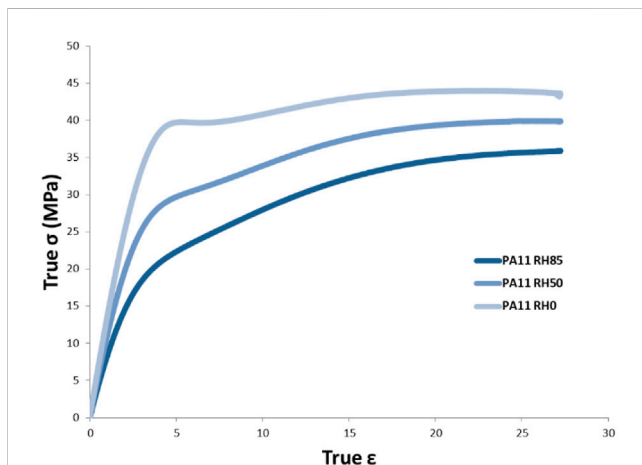

FIGURE 8
Global true stress vs. true strain for the tensile test of PA11 for RH0, RH50, and RH85 at 23°C.

process (Shubhalakshmi et al., 2016), (Singha, 2012) has good mechanical stability like glass fiber, a considerable dispersion is noticed for its different mechanical properties (E11, E22, and G12). This is related to manufacturing defects; a deviation in the orientation of fibers for the composite UD basalt/PA11 composite was found.

The hybridization of flax and basalt fibers created a synergy that allowed a lower dispersion of the mechanical properties of the hybrid5050/PA11 composite. In conclusion, the dispersion depends on the nature of the fibers, the type of fabric (UD or twill) and the orientation of the composite.

The second phase of the experimental study investigates the effect of moisture on the evolution of the mechanical behaviour of our materials, the matrix PA11, flax/PA11, basalt/PA11 and Hybrid 5,050/PA11 composites. This part aims to understand and quantify the evolution of the mechanical properties of materials for the three humidity levels RH0, RH50 and RH85. Then, it will enable to verify the interest of hybridization in reducing the material's sensitivity to humidity.

Figure 8 shows the typical response of the PA11 matrix during quasi-static tensile tests for the three moisture levels RH0, RH50, and RH85.

The different Young's moduli of PA11 are reported in Supplementary Table S4. They show that moisture promotes the plasticization of the material and reduces stiffness.

Figure 9 shows the evolution of the mechanical properties of flax/PA11, hybrid5050/PA11 and basalt/PA11 for the three moisture levels RH0, RH50 and RH85:

From the values in Table 4, it can be seen that there is a decrease in the mechanical properties of the different composites. The Flax/PA11 composite shows a similar significant decrease in its mechanical properties for RH50 and RH85. The longitudinal modulus E11 decreases from 10,100 MPa (RH0) to 7,918 MPa for RH50 and 5,001 MPa for RH85, i.e., a decrease of 21% for RH50% and 50% for RH85. This decrease can be explained by the sensitivity of both the flax fiber (Bourmaud and Baley, 2009), (Abida et al., 2020), (Fabre et al., 2017) and the PA11 matrix (Destaing et al., 2016). The evolution of the properties of flax fiber is related to its microscopic structure. The matrix is mainly composed of hemicellulose and lignin. The cellulose fibrils are helically oriented at the microfibril angle (Supplementary Figure S3). The physical properties of natural fibers are mainly determined by their chemical and physical composition, structure, percentage of cellulose, microfibril angle, cross-section and degree of polymerization. The lower the microfibrillar angle, the higher the stiffness and strength of the fiber; the higher the microfibrillar angle, the higher the elongation at break. It can be seen that the microfibrillar angle increases with increasing humidity, which explains the evolution of the stiffness of the flax/PA11 composite.

For the hybrid5050/PA11 composite, a moderate decrease in mechanical properties as a function of humidity was observed compared to the flax/PA11 composite. Indeed, for the longitudinal Young's modulus E11 a decrease of 7% at RH50% and 27% at RH85; the basalt fiber has considerably reduced the hybrid5050/PA11 sensitivity to moisture, as shown in Table 4.

A comparison of the mechanical properties of the studied composites for the different moisture contents is represented in Figure 10.

Although the basalt fiber has a good moisture sensitivity (Rozycki et al., 2018), its mechanical properties were reduced for RH50 and RH85 compared to the dry state RH0 (Figure 10). E11 drops from 23,300 MPa (RH0) to 17,893 MPa (RH50) and 19,570 MPa for RH85. For the basalt/PA11 composite, the variation in mechanical properties essentially depends on the sensitivity of PA11 to humidity, bearing in mind that fiber content (27%) is relatively low (Coussa et al., 2017). However, an improvement in the mechanical properties was observed from RH50 to RH85 in all directions (0°, 45°, and 90°). The improvement in the mechanical properties of the basalt/PA11 composite at RH85 could be related to a modification of the fiber/matrix interface, which could allow a better adhesion between the basalt fiber and the PA11 matrix.

Following the mechanical characterisation tests of the different materials studied, a microscopic study was conducted using a Scanning Electron Microscope (Figure 11). There are different damage mechanisms for composite materials depending on the nature of the fibres, the matrix and the fabric used. The damage modes are fibre breakage, fibre/matrix debonding and matrix
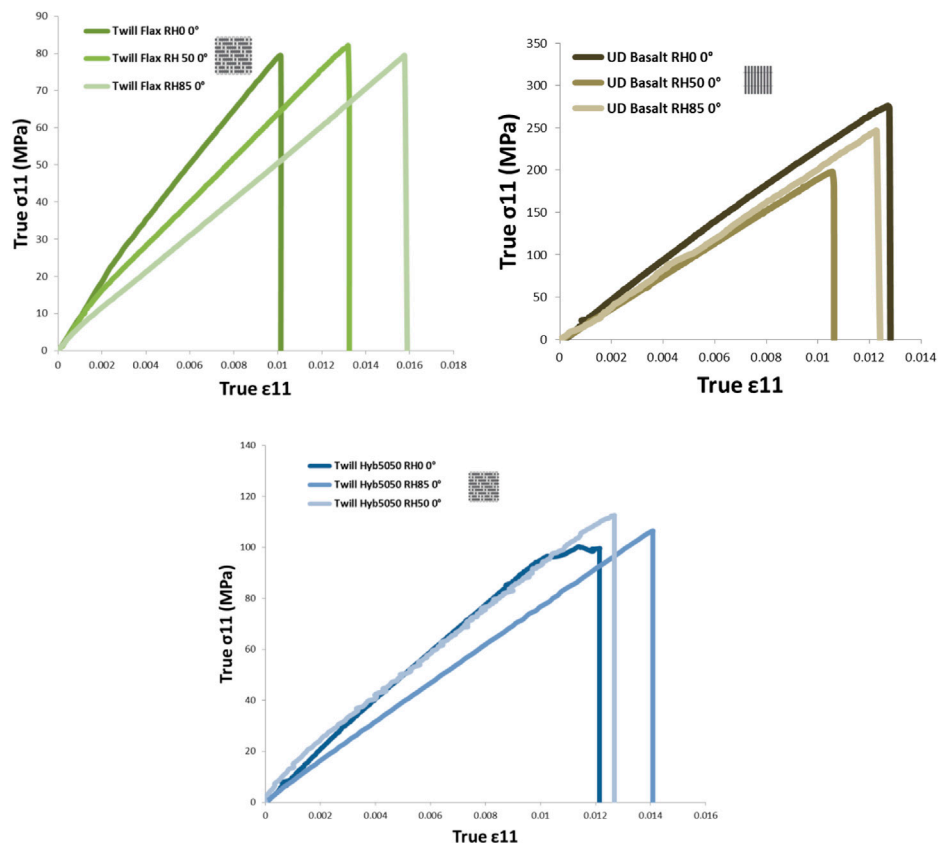
FIGURE 9
Global true stress vs. true strain for the tensile tessof flax/PA11, hyb5050/PA11 and basalt/PA11 0° for RH0 RH50 and RH85 at 23°C.

cracking. The analysis of the SEM results (Figure 12) shows that fibre breakage as the damage mode for the flax/PA11 composite is fibre breakage and fibre/matrix delamination for the basalt/PA11 composite. These damage modes were retained for the hyb5050/PA11 composites.

Numerical study

The second part of the research work is devoted to the numerical study based on homogenization methods; it allows the prediction of the mechanical behaviour of a heterogeneous material from the mechanical properties of its phases. It will be able to determine the effective properties at the macroscopic scale of the material from a Representative Elemental Volume (REV) that depends on the scale of hybridization. In this study, a numerical method based on a multi-scale homogenization (Supplementary Figure S4) will be used to capture the geometrical features of the materials under study and to integrate the hygrometry that impacts the behaviour of the composite.

The multi-scale numerical homogenization method is divided into two phases. The first phase concerns the homogenization of the constituents (fiber and matrix) at the microscopic scale. It provides the behaviour of the polymer reinforced by the fiber tow. The second phase represents homogenization at the macroscopic scale (fiber tow

and matrix). It allows having the behaviour of the studied composite (Rozycki et al., 2018). Initially, the elastic phase of the composite material's mechanical behavior is studied. Therefore, this part focuses on the determination of the effective properties for the following composite materials: flax/PA11 (twill), basalt/PA11 (UD), and hybrid5050/PA11 (twill) for RH0.

Multiscale Designer, developed by Altair, is used as a numerical homogenization tool to predict effective properties (Altair Multiscale Designer User Manual, 2021). Macro homogeneous linear material properties are calculated using either a forward homogenization problem (Yuan and Fish, 2008) or an inverse optimization problem. It allows the prediction of the mechanical properties of different types of composite (UD, twill, etc.) from the intrinsic properties of their fiber and matrix components and their spatial distribution. This tool allows different types of REV to be represented, depending on the composite studied (UD, twill, with or without the fiber/matrix interface) (Supplementary Figure S5) and uses the periodic boundary conditions.

The REV type (Supplementary Figure S5) was chosen for its ability to integrate two different fibers (flax and basalt fiber) to represent a hybrid composite. The first numerical study is carried out without adding an interface between the matrix and fibers due to the lack of information on their mechanical properties.

The REV dimensions were defined from the micrographic inspection of the different composite materials (Supplementary
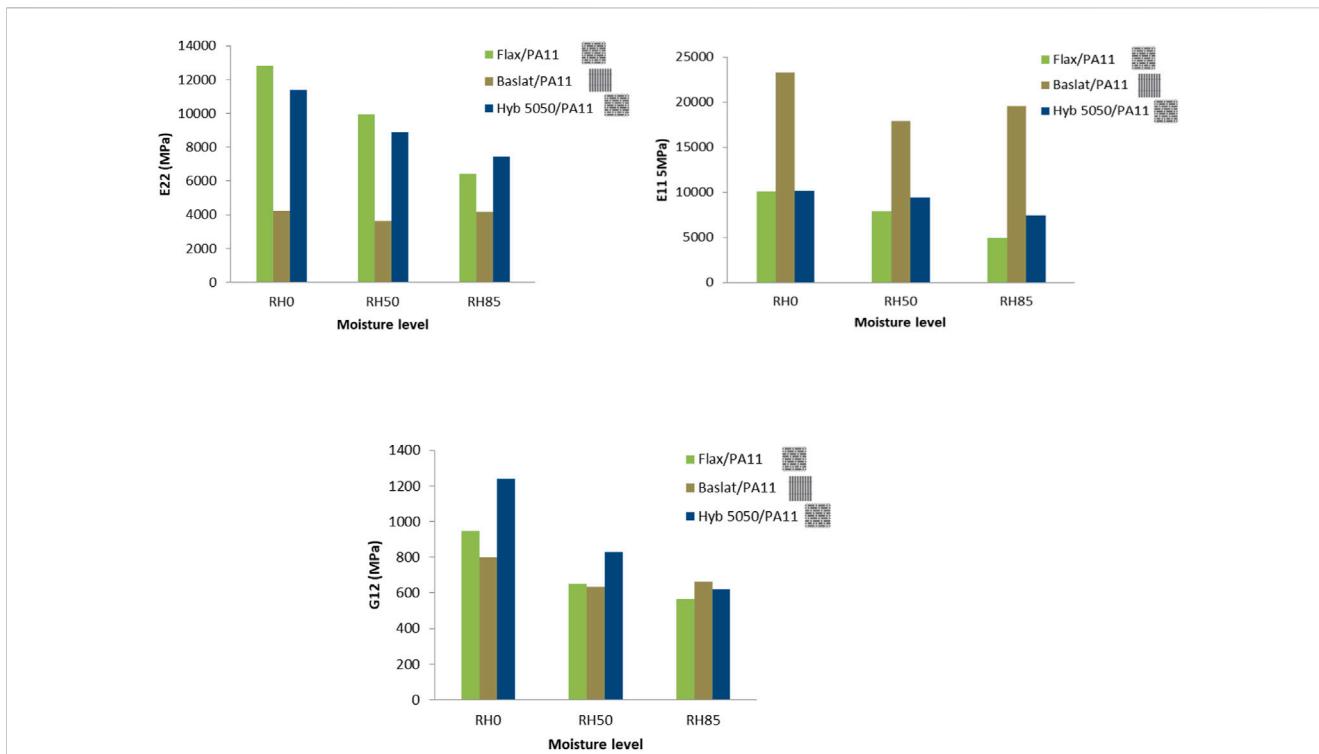
FIGURE 10

Comparison of the mechanical properties E11, E22 and G12 for flax/PA11, basalt/PA11 and hybrid 5,050/PA11 composites, for RH0, RH50 and RH85 at 23°C.

FIGURE 11

Scanning electron microscope (SEM).

Figure S6) using the image processing tool Image J. The following dimensions were determined: Tow major radius ry, Tow minor radius rz and Tow spacing sy (Supplementary Figure S7).

Supplementary Figure S7 presents the different REV dimensions for the flax/PA11 composite: the tow major radius (ry), the minor tow radius (rz), the tow spacing (sy) and the fiber volume fraction (Vf). This unit cell does not include the crimp of the twill weave.

The multi-scale homogenization was carried out using the intrinsic properties of flax fibers, basalt fibers and PA11 (Table 1) according to their volume fractions and arrangements (Table 2). The indices 1, 2, and 3 refer to the main axes of the fiber, with axis 1 referring to the direction of the fiber (Baley et al., 2017).

These numerical simulations will be used to compare and correlate the numerical results with the experimental results. In order to make a consistent comparison between the different composite materials, The experimental characterization tests will be extended by studying the composites with an identical fiber content and similar weave (Vf of 42% and balanced twill). Supplementary Table S6 shows the different materials that will be examined using the homogenization method.

The numerical and experimental results are compared in Table 5. The error between the numerical and experimental results is calculated from:

$$Error = \frac{Experimental - Numerical}{Experimental} \quad (7)$$

A significant difference was found between the experimental and numerical properties, reflected in a high error value for all the flax/PA11, basalt/PA11 and hybrid5050/PA11 composites. This can be explained by the limitation of including the fiber/matrix interface and the flax/basalt interface for the hybrid composite (Destaing et al., 2016). The type of VER has a strong influence on the numerical results. On the other hand, a difference could be
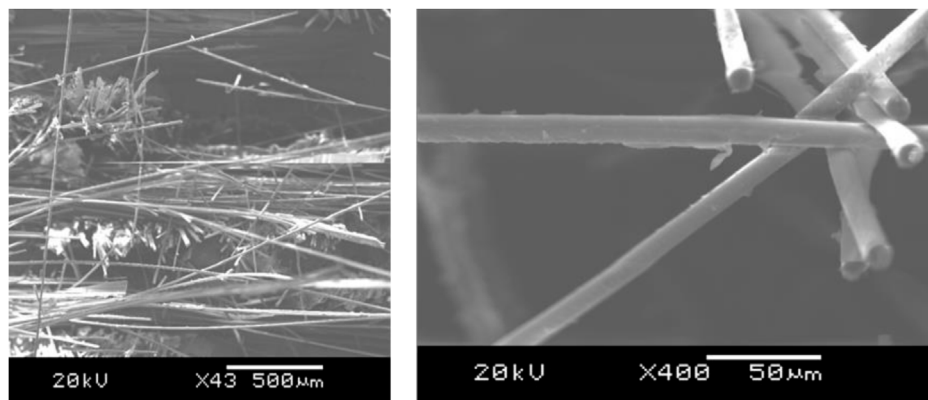
Flax/PA11 specimen
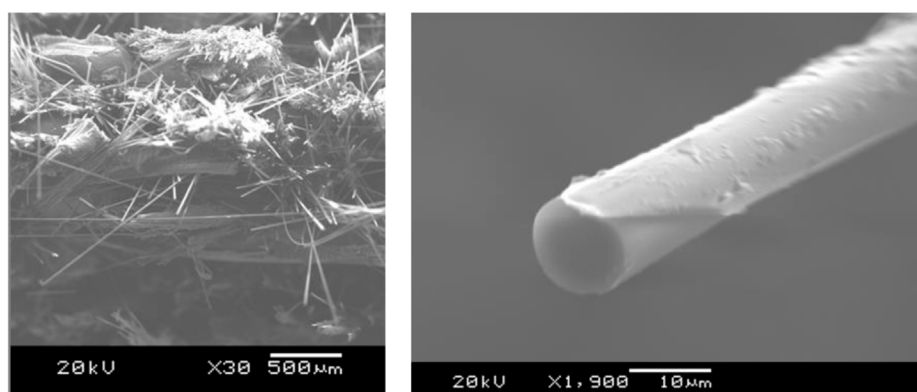
Basalt/PA11 specimen

FIGURE 12
SEM view of flax/PA11 and Basalt/PA11 composites after 0˚ quasi-static tensile tests.

TABLE 1 Mechanical properties of flax and basalt fibers and the PA11 matrix for RH0 The description of the different composite materials is shown in Table 2.

Mechanical properties	Basalt (Dhand et al., 2015)	Flax (Baley et al., 2017)	PA11 (Destaing et al., 2016)
Longitudinal Young's modulus E_{f_1} (MPa)	89,000	52,000	1,400
Transverse Young's modulus E_{f_2} (MPa)	—	8,000	—
Longitudinal shear modulus $G_{f_{12}}$ (MPa)	—	2,410	—
Transverse shear modulus $G_{f_{23}}$ (MPa)	—	2,930	—
Poisson's ratio	0.2	0.4	0.06
Density (g/cm3)	2.7	1.4	1.03

TABLE 2 Fiber volume fraction and density of the studied composites.

	Flax/PA11	Basalt/PA11	Hyb5050/PA11
Vf (Vol.)	42%	27%	33%
Density (g/cm³)	1.18	1.48	1.36
Fabric	Twill	UD	Twill

observed between the intrinsic mechanical properties of the materials used and the values available in the bibliography.

Then we were interested in the mechanical behaviour of the composite for the linear elastic and the non-linear parts. Predefined constitutive law in Multiscale Designer (Rate-independent plasticity (RI) model) was used to represent the stress-strain curve for PA11 using the constitutive model in Eq. 8
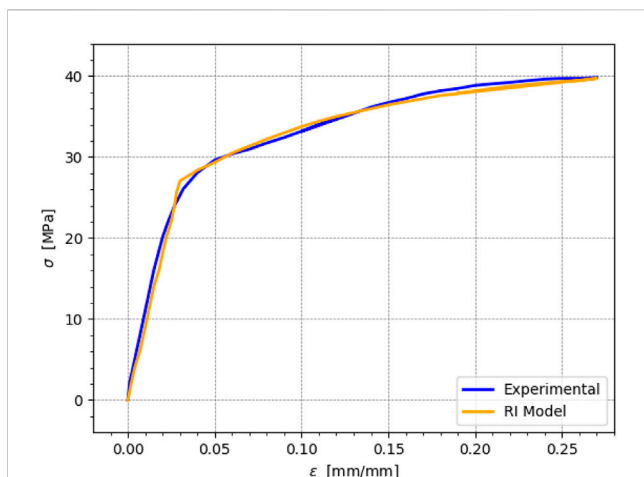
FIGURE 13
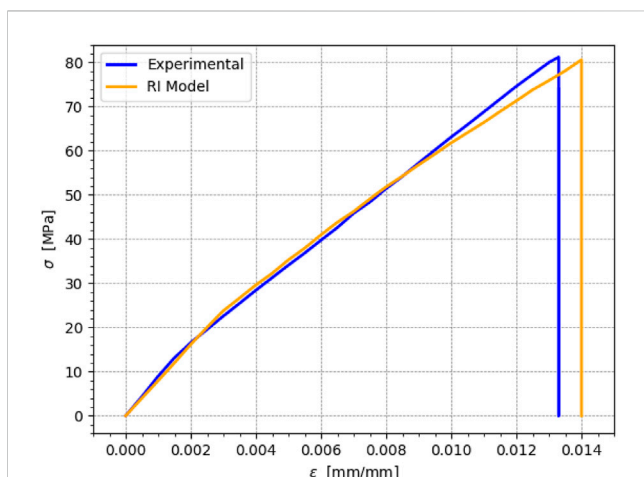Comparative curves of experimental results and numerical simulation for PA11 at RH50.

FIGURE 14
Comparative curves of experimental results with numerical simulation for flax/PA11 (0° and RH50).

$$\sigma = \sigma_y + \left(\sigma_1 - \sigma_y\right)\left[1 - e^{-\delta\left(\varepsilon - \frac{\sigma}{E}\right)}\right] + H\left(\varepsilon - \frac{\sigma}{E}\right) \qquad (8)$$

Where σ_y is the yield strain, σ_1 is the ultimate strain , H is the linear term for the hardening law and δ is the exponent for the evolution law.

This model provides a good fit for the experimental data, as shown in Figure 13.

An inverse homogenization was performed to determine the mechanical properties of the flax fiber from the experimental curves. Table 6 shows the mechanical properties of the flax fiber at RH0, RH50, and RH85.

These fiber properties are used to perform a numerical homogenization and to verify the correlation between the RI model and the experimental results at RH 50° and 0° direction at ambient temperature. Figure 14 shows good agreement between the experiment and model.

To achieve our study on the effect of hybridization on the evolution of the mechanical behavior for the hybrid composite, a focus on the different types of hybridization was made, which depends on the scale of hybridization. In fact, there are three scales of hybridization: the laminate scale, the layer scale by co-weaving and the fiber scale by commingling two different fibers. Most of the research to date has focused on the study of hybrid laminates. Initial work has focused on analyzing hybrid layer scale composites; studying the other scales will allow the best type of hybridization for better mechanical properties. A specific REV was developed on Hypermesh for each scale of hybridization presented in Supplementary Figure S8.

The effective properties of the hybrid composites are presented in Table 6.

The numerical simulations show that the hybrid composite made of commingled fibres and the hybrid co-woven composite have the same mechanical properties. In fact, the hybridization is carried out in the same layer. Only the distribution of the fibres in the same layer was modified with an equal distribution in the longitudinal and transverse directions. The behaviour of the composite is balanced in both directions of the material. However, the results show a difference in the mechanical properties of the laminated composite with the mixed fibre composite and the co-woven composites. The longitudinal properties are also different from the transverse properties. This difference is related to the nature of the fabrics, in fact a combination of flax twill and basalt UD layer was used. These results show the effect of the nature of the hybridization on the mechanical properties of the hybrid composite material.

Results and discussion

The results were analyzed with the aim of understanding the benefits of hybridization by comparing the three composite materials flax/PA11, basalt/PA11 and hybrid5050/PA11. The second part was dedicated to the impact of hygrometry on the evolution of the mechanical behaviour of the different composites materials for three moisture levels RH0, RH50 and RH85. Finaly, a comparaison of hybridization levels was analyzed using multi scale homogenization. The different mechanical behaviors of the flax/PA11, basalt/PA11 and hyb5050/PA11 composites are presented in Figure 5 and their mechanical properties are reported in Table 3. As expected the basalt/PA11 composite is stiffer than the hybrid 5,050/PA11 and flax/PA11 composites for the 0° direction due to the high mechanical properties of the basalt fiber (Singha, 2012). The hybridization has improved the mechanical characteristics of the hybrid 5,050/PA11 compared to the flax/PA11 composite. The hybrid composite is 20% stiffer than the flax composite (Figure 4). Furthermore, Figure 7 shows that the hybrid5050/PA11 composite has a lower dispersion of Young's modulus

TABLE 3 Mechanical characteristics of Hybrid5050/PA11, basalt/PA11 and flax/PA11 composites for RH0 and for directions (0˚/45˚/90˚) at 23˚C.

		Flax		Basalt		Hyb 50 50	
0˚		E11(MPa)	υ 12	E11(MPa)	υ 12	E11(MPa)	υ 12
		10,100 ± 1,340	0.04 ± 0.02	23,300 ± 3900	0.18 ± 0.02	10,220 ± 650	0.05 ± 0.05
		σ 11 failure (MPa)	ε 11 failure	σ 11 failure (MPa)	ε 11 failure	σ 11 failure (MPa)	ε 11 failure
		60 ± 11	0.008 ± 0.01	255 ± 37	0.01 ± 0.001	70 ± 17	0.01 ± 0.04
90˚		E22(MPa)	υ 21	E22(MPa)	υ 21	E22(MPa)	υ 21
		12,807 ± 1,200	0.05 ± 0.153	4,220 ± 545	0.032 ± 0.07	11,400 ± 680	0.50 ± 0.2
		σ 22 failure (MPa)	ε 22 failure	σ 22 failure (MPa)	ε 22 failure	σ 22 failure (MPa)	ε 22 failure
		75 ± 4	0.007 ± 0.002	57 ± 4	0.015 ± 0.01	85 ± 3	0.008 ± 0.0003
45˚		G12(MPa)		G12(MPa)		G12(MPa)	
		949 ± 143		801 ± 156		1,240 ± 150	
		σ 12 failure (MPa)	2 ε 12 failure	σ 12 failure (MPa)	2 ε 12 failure	σ 12 failure (MPa)	2 ε 12 failure
		35 ± 5	0.06 ± 0.032	54 ± 10	0.14 ± 0.04	55 ± 5	0.1 ± 0.02

E11, Longitudinal elastic modulus; E22, Transverse elastic modulus; G12, Shear modulus; σ 11 failure; Longitudinal stress at break; ε 11 failure, Longitudinal strain at break; σ 22 failure, Transverse stress at break; ε 22 failure, Transverse strain at break; σ 12 failure, Shear stress at break; 2 ε 12 failure, Shear strain at break; υ 12, Poisson coefficient 12; υ 21, Poisson coefficient 21.

TABLE 4 Young Modulus of hyb5050/PA11, basalt/PA11 and flax/PA11 composites for RH0, RH50 &RH85 and for directions (0˚/45˚/90˚) at 23 ˚C.

		Flax/PA11	Baslat/PA11	Hybrid5050/PA11
RH0	E11(MPa)	10,100 ± 1,340	23,300 ± 3900	10,220 ± 650
	E22(MPa)	12,807 ± 1,200	4,220 ± 545	11,400 ± 680
	G12(MPa)	949 ± 143	801 ± 156	1,240 ± 150
RH50	E11(MPa)	7,918 ± 1,295	17,893 ± 3402	9,440 ± 392
	E22(MPa)	9,950 ± 1,000	3619 ± 443	8,886 ± 401
	G12(MPa)	650 ± 284	632 ± 310	828 ± 90
RH85	E11(MPa)	5,001 ± 479	19,570 ± 1,481	7,462 ± 360
	E22(MPa)	6,434 ± 1,061	4,191 ± 397	7,428 ± 175
	G12(MPa)	566 ± 231	664 ± 91	623 ± 62

The evolution of the mechanical properties of flax/PA11, hybrid5050/PA11 and basalt/PA11 for the three moisture levels RH0, RH50, and RH85 is presented in Figure 9. Table 4 shows a decrease in the mechanical properties of the different composites. The Flax/PA11 composite had a significant loss of its mechanical properties for RH50 and RH85. For the hybrid5050/PA11 composite, a moderate modification in mechanical properties was observed compared to the flax/PA11 composite. Indeed, for the longitudinal Young's modulus E11 a decrease of 7% at RH50% and 27% at RH85.

For the multiscale homogenization a comparison between numerical and experimental results was reported in Table 5 through error calculation. High error value was observed for all the flax/PA11, basalt/PA11 and hybrid5050/PA11 composites. The first explanation is related to the limitation of including the fiber/matrix interface and the flax/basalt interface for the hybrid composite (Destaing et al., 2016). Also, VER size and type have a strong influence on the numerical results. On the other hand, the difference between the intrinsic mechanical properties of the materials used and the values available in the bibliography could be observed. For the hybridization levels, the effective properties of the hybrid composites are presented in Table 6. The hybrid composite made of commingled fibres and the

versus basalt/PA11 and flax/PA11 composites for the different directions (0˚, 45˚, and 90˚). Using flax and basalt fibers provided a synergy wich reduces the dispersion of the mechanical properties of the hybrid5050/PA11 composite.

TABLE 5 Comparative table of numerical/experimental mechanical properties of Flax/PA11, basalt/PA11, hyb5050/PA11 composites for RH0.

	Flax			Basalt			Hybrid5050		
	E11	E22	G12	E11	E22	G12	E11	E22	G12
Experimental (MPa)	10,100	12,807	949	23,283	4,220	801	10,218	11,395	1,240
Numerical (MPa)	9,970	9,970	1,090	25,060	2,204	1,040	15,000	15,000	1,090
Error %	1.3	22	−15	−8	47	−30	−47	−32	12

TABLE 6 Numerical simulation results for different hybrid composite materials.

	E11 (MPa)	E22 (MPa)	G12 (MPa)
Comminglingfibers	15,000	15,000	1,090
Co-weaving	15,000	15,000	1,090
Laminating	18,800	6,140	1840

hybrid co-woven composite have the same mechanical properties. In fact, the hybridization is carried out in the same layer.

Conclusion and references

The main objective of this study is to highlight the interest in using biocomposite materials in structural parts by understanding their mechanical behaviour.

Firstly, natural fibers and thermoplastic matrices were studied to determine the best fibre/matrix combination. The thermo-compression parameters, i.e., temperature, dwelltime and pressure were then validated to meet the industrial requirements. The second phase was devoted to the experimental characterization of the different flax, basalt and hybrid composites and the PA11 matrix. This part aimed to identify the mechanical properties of the studied materials in the dry state and at room temperature, then the influence of humidity on the evolution of the mechanical properties of the matrix and the different flax/PA11, basalt/PA11 and hybrid5050/PA11composites was analyzed. The results of the characterization tests highlight the interest of hybridization. Indeed, the use of basalt fibers with flax fibers improves the mechanical performance of the hybrid composite compared to the flax/PA11 composite and reduces its density by increasing the potential mass gain compared to the basalt/PA11 composite. Furthermore, the hybridization allowed a significant reduction in the scatter of the mechanical properties of the hybrid5050/PA11 compared to the flax/PA11 and the basalt/PA11 composites. The results of the experimental study are in agreement with those obtained in published research works. Indeed, hybridization improves the mechanical performance of the hybrid composite and reduces its sensitivity to moisture, especially when a plant fibre is combined with a synthetic fibre that has a low moisture absorption (Nasimudeen et al., 2021), (Jeyaguru et al., 2022b), (Jeyaguru et al., 2022d), (Jeyaguru et al., 2023). The research work of (Almansour et al., 2017; Almansour et al., 2018) approved that positive impact of using basalt fibres with flax/vinylester compositeon the interlaminar fracture toughness. Basalt fibres enhance the durability and limited the sensitivity of flax fibres. Likewise, (Fiore et al., 2016), confirmed and prove a better durability for an hybrid composite with two external basalt layers. (Raponi et al., 2022). shows that the intraply arrangement of flax and basalt was especially useful in improving the tensile properties of flax-based laminates by 116% and 69% for ultimate strength and modulus.

In the second part of this paper, the multiscale numerical homogenization approach is used to determine the effective properties of the studied materials and to compare the numerical results with the experimental values. It also allowed to understand the influence of hygrometry on the composite behaviour and to complete our empirical study by homogenizing new composite

materials with identical fiber content and weave. The significant discrepancy requires the study and the integration of the fiber-matrix interface and the verification of the intrinsic properties of the flax fiber through a reverse homogenization based on the experimental curves. It helped to understand the effect of moisture on the mechanical behaviour of plant fibres. The numerical tool allows us to compare the three scales of hybridization; the laminate scale, the layer scale (by co-weaving) and the fibre scale (by blending two different fibres), and helps us to make the appropriate choice of hybridization for the intended application.

Data availability statement

The original contributions presented in the study are included in the article/Supplementary Material, further inquiries can be directed to the corresponding author.

Author contributions

WG: carried out experimental and numerical works, wrote the draft paper. CB and PR: contributed to conception and design of the study, contributed to manuscript revision, read, and approved the submitted version. All authors contributed to the article and approved the submitted version.

Acknowledgments

Conflict of interest

WG was employed by the company Department Body in White Research and Innovation Unit, Bertrandt.

The remaining authors declare that the research was conducted in the absence of any commercial or financial relationships that could be construed as a potential conflict of interest.

Publisher's note

Supplementary material

The Supplementary Material for this article can be found online at: https://www.frontiersin.org/articles/10.3389/fmats.2023.1176408/full#supplementary-material

References

Abida, M., Gehring, F., Mars, J., and Vivet, A. (2020). Hygro-mechanical coupling and multiscale swelling coefficients assessment of flax yarns and flax/epoxy composites, *Compos. Part A Appl. Sci. Manuf.* 136. doi:10.1016/j.compositesa.2020.105914

Almansour, F. A., Dhakal, H. N., and Zhang, Z. Y., (2017), Effect of water absorption on Mode I interlaminar fracture toughness off lax/basalt reinforced vinylester hybrid composites. *Compos Struct.*, 168:813–825. doi:10.1016/j.compstruct.2017.02.081

Almansour, F. A., Dhakal, H. N., and Zhang, Z. Y. (2018). Investigation into Mode II interlaminar fracture toughness characteristics of flax/basalt reinforced vinyl ester hybrid composites. *Compos Sci. Technol.* 154, 117–127. doi:10.1016/j.compscitech.2017.11.016

Altair Multiscale Designer User Manual, 2021.

Athith, D., Sanjay, M. R., Gowda, Y., Madhu, P., Arpitha, G. R., Yogesha, B., et al. (2018). Effect of tungsten carbide on mechanical and tribological properties of jute/sisal/E-glass fabrics reinforced natural rubber/epoxy composites. *J. Industrial Text.* 48, 713–737. doi:10.1177/1528083717740765

Baley, C., and Bourmaud, A. (2014). Average tensile properties of French elementary flax fibers. *Mater Lett.* 122, 159–161. doi:10.1016/j.matlet.2014.02.030

Baley, C., and Bourmaud, A. (2014). Average tensile properties of French elementary flax fibers. *Mater. Lett.* 122, 159–161. doi:10.1016/j.matlet.2014.02.030

Baley, C., Bourmaud, A., and Scida, D. (2017). Influence of the scattering of flax fibres properties on flax/epoxy woven ply stiffness. *Mater. Des.* 122, 136–145. doi:10.1016/j.matdes.2017.02.094

Baley, C., Morvan, C., and Grohens, Y. (2005). «Influence of the absorbed water on the tensile strength of flax fibers». *Macromol. Symp.* 222, p195–p202. doi:10.1002/masy.200550425

Barbulée, A., Jernot, J. P., Bréard, J., and Gomina, M. (2014). Damage to flax fibre slivers under monotonic uniaxial tensile loading. *Compos. Part A Appl. Sci. Manuf.* 64, 107–114. doi:10.1016/j.compositesa.2014.04.024

Bourmaud, A., and Baley, C. (2007). Investigations on the recycling of hemp and sisal fibre reinforced polypropylene composites. *Polymdegr. Stab.* 92, 1034–1045. doi:10.1016/j.polymdegradstab.2007.02.018

Bourmaud, A., and Baley, C. (2009). Rigidity analysis of polypropylene/vegetal fibre composites after recycling. *PolymDegradStab* 94, 297–305. doi:10.1016/j.polymdegradstab.2008.12.010

Chandrasekar, M., Shahroze, R. M., Senthil Muthu Kumar, T., Senthilkumar, K., Ishak, M. R., Rajini, N., et al. (2022). Influence of a silica aerogel filler on the mechanical, thermal, and physical properties of flax/epoxy composite. *Mech. Compos. Mater.* 58 (N°2), 383–396.

Chandrasekar, M., Siva, I., Kumar, T. S. M., Senthilkumar, K., Siengchin, S., and Rajini, N. (2020). Influence of fibre inter-ply orientation on the mechanical and free vibration properties of banana fibre reinforced polyester composite laminates. *J. Polym. Environ.* 28, 2789–2800. doi:10.1007/s10924-020-01814-8

Coussa, et al. (2017). Influence of rate effects on the mechanical behaviour of thermoplastic matrix woven composites. *JNC 20–Ecole Des. PontsParisTech.*

Destaing, F., Jouannot-Chesney, P., Gomina, M., and Bréard, J. (2016). Choice between film or powder of PA11 for processing flax fiber reinforced composites. *Revue des Compos. des MatériauxAvancés n°3* 26, 435–449. doi:10.3166/rcma.26.435-449

Dhand, V., Mittal, G., Rhee, K. Y., Park, S. J., and Hui, D. (2015). A short review on basalt fiber reinforced polymer composites. *Composites:Part B*, 166–180.

El Hadi, S., Scida, D., Pac, M. J., and Ayad, R. (2019). Mode-I interlaminar fracture toughness of flax, glass and hybrid flax-glass fibre woven composites: Failure mechanism evaluation using acoustic emission analysis. *Polym. Test.* 75, 246–253. doi:10.1016/j.polymertesting.2019.02.022

Fabre, V., Quandalle, G., Billon, N., and Cantournet, S. (2017). Time-Temperature-Water Content equivalence on dynamic mechanical response of polyamide 6. *Polymer* (6), 2–3.

Fargassa, C., Pavlovic, A., and Santulli, C. (2018). Mechanical and impact characterization of flax and basalt fibervinylester composites an their hybrids. *Compos. Part B* 137, 247–259.

Fiore, V., Calabrese, L., Di Bella, G., Scalici, T., Galtieri, G., Vakenza, A., et al. (2016). Effects of aging in salt spray conditions on flax and flax/basalt reinforced composites: Wettability and dynamic mechanical properties. *Compos. B* 93, 35–42. doi:10.1016/j.compositesb.2016.02.057

Fragassa, C., Santulli, C., Pavlović, A., and &Šljivić, M. (2015). Improving performance and applicability of green composite materials by hybridization. *Contemp. Mater.* 6, 35–43. doi:10.7251/comen1501035f

Jeyaguru, S., Thiagamani, S. M. K., Pulikkalparambil, H., Siengchin, S., Krishnasamy, S., Muthukumar, C., et al. (2022). Mechanical, absorption, and swelling properties of jute/kenaf/banana reinforced epoxy hybrid composites: Influence of various stacking sequences. *Polym. Compos.* 43, 8297–8307. doi:10.1002/pc.26999

Jeyaguru, S., Thiagamani, S. M. K., Pulikkalparambil, H., Siengchin, S., Krishnasamy, S., Muthukumar, C., et al. (2022). Mechanical, acoustic and vibration performance of intra-ply Kevlar/PALF epoxy hybrid composites: Effects of different weaving patterns. *Polym. Compos.* 43, 3902–3914. doi:10.1002/pc.26665

Jeyaguru, S., Thiagamani, S. M. K., Pulikkalparambil, H., Siengchin, S., Krishnasamy, S., Rajkumar, A. G., et al. (2022). Effects of different weaving patterns on thermomechanical and dynamic mechanical properties of Kevlar/pineapple leaf fiber hybrid composites. *Polym. Compos.* 43, 4979–4997. doi:10.1002/pc.26764

Jeyaguru, S., Thiagamani, S. M. K., Pulikkalparambil, H., Siengchin, S., Subramaniam, J., Rangappa, S. M., et al. (2022). Mechanical, acoustic and vibration performance of intra-ply kevlar/PALF epoxy hybrid composites: Effects of different weaving patterns. *Polym. Compos.* 43, 3902–3914. doi:10.1002/pc.26665

Jeyaguru, S., Thiagamani, S. M. K., Rangappa, S. M., and Siengchin, S. (2023). Experimental studies on the absorption, swelling and erosion performance of hybrid woven Kevlar/hemp reinforced epoxy composites. *Express Polym. Lett.* 17 N°4, 353–372. doi:10.3144/expresspolymlett.2023.26

Kumar, T. S. M., et al. (2020). *Influence of fillers on the thermal and mechanical properties of biocomposites: An overview, biofibers and biopolymers for biocomposites.* Springer, 111–133.

Mohit, H., Rangappa, S. M., Siengchin, S., Gorbatyuk, S., Manimaran, P., Alka Kumari, C., et al. (2022). A comprehensive review on performance and machinability of plant fiber polymer composites. *Polym. Compos.* 43, 608–623. doi:10.1002/pc.26403

Nasimudeen, N. A., Karounamourthy, S., Selvarathinam, J., Thiagamani, S. M. K., Pulikkalparambil, H., Krishnasamy, S., et al. (2021). Mechanical, absorption, and swelling properties of Vinyl Ester based natural fibre hybrid composite. *Appl. Sci. Eng. Prog.* 14 N°4, 680–688.

Petrucci, P., Santulli, C., Puglia, D., Sarasini, F., Torre, L., and Kenny, J. M. (2013). Mechanical characterisation of hybrid composite laminates based on basalt fibres in combination with flax, hemp and glass fibres manufactured by vacuum infusion. *Mater. Des.* 49, 728–735. doi:10.1016/j.matdes.2013.02.014

Rangappa, S. M., Siengchin, S., Parameswaranpillai, J., Jawaid, M., and Ozbakkaloglu, T. (2022). Lignocellulosic fiber reinforced composites: Progress, performance, properties, applications, and future perspectives. *Polym. Compos.* 43, 645–691. doi:10.1002/pc.26413

Raponi, E., Boria, S., Giammaria, V., Fischer, B., Pörnbacher, J., Sarasini, F., et al. (2022). Effect of basalt intraply hybridization on the damage tolerance of flax laminates: Experimental analysis and analytical modeling under low-velocity impact. *Compos. Struct.* 287, 115270. doi:10.1016/j.compstruct.2022.115270

Rozycki, P., Mbacke, M., and Dau, A. (2018). *Multiscale homogenization of a glass-PA66 fabric composite behaviour for crash studies, ECCM18-18th European conference on composite materials*, 24–28.

Sanjay, M. R., Madhu, P., Jawaid, M., Senthamaraikannan, P., Senthil, S., and Pradeep, S. (2018). Characterization and properties of natural fiber polymer composites: A comprehensive review. *J. Clean. Prod.* 172, 566–581. doi:10.1016/j.jclepro.2017.10.101

Senthilkumar, K., Rajini, N., Saba, N., Chandrasekar, M., Jawaid, M., and Siengchin, S. (2019). Effect of alkali treatment on mechanical and morphological properties of pineapple leaf fibre/polyester composites. *J. Polym. Environ.* 27, 1191–1201. doi:10.1007/s10924-019-01418-x, No.

Senthilkumar, K., Subramaniam, S., Ungtrakul, T., Kumar, T. S. M., Chandrasekar, M., Rajini, N., et al. (2022). Dual cantilever creep and recovery behavior of sisal/hemp fibre reinforced hybrid biocomposites: Effects of layering sequence, accelerated weathering and temperature. *J. Industrial Text.* 51, 2372S–2390S. doi:10.1177/1528083720961416

Shahroze, R. M., Chandrasekar, M., Senthilkumar, K., Senthilmuthukumar, T., Ishak, M. R., and Asyraf (2019). A review on the various fibre treatment techniques used for the fibre surface modification of the sugar palm fibres. *Proc. Seminar Enau Kebangsaan*, 48–52.

Shubhalakshmi, B. S., Jagannatha Reddy, H. N., and Arjun, K. (2016). *International journal of engineering sciences and research technology*, 2277–9655. ISSN,p.

Singha, K. (2012). A short review on basalt fiber. *Int. J. Text. Sci.*, 19–28.

Swolfs, Y., Verpoest, I., and Gorbatikh, L. (2019). Recent advances in fibre-hybrid composites: Materials selection, opportunities and applications. *Int. Mater. Rev.* 64, 181–215. doi:10.1080/09506608.2018.1467365

Swolfs, Y., Gorbatikh, L., and Verpoest, I. (2014). *Fiber hybridization in polymer composites: A review, composite Part A: Applied science and manufacturing*, 181–200.

Toumis, R. B., Renard, J., Monin, M., and Nimdum, P. (2013). Fatigue damage modelling of continuous E-glass fibre/epoxy composite. *Procedia Eng.* 66, 723–736. doi:10.1016/j.proeng.2013.12.126

Yuan, Z., and Fish, J. (2008). Toward realization of computational homogenization in practice. *Int. J. Numer. Methods Eng.* 73 (3), 361–380. doi:10.1002/nme.2074